Journal of the Ceramic Society of Japan 118 [5] 370-373 2010 Paper

Fabrication of large-area silica colloidal crystals immobilized in hydrogel film

Toshimitsu KANAI,[*,] Tsutomu SAWADA[*,†] and Junpei YAMANAKA[***]**

[*]National Institute for Materials Science, 1–1, Namiki, Tsukuba, Ibaraki 305–0044
[**]Yokohama National University, 79–5, Tokiwadai, Hodogaya, Yokohama, Kanagawa 240–8501
[***]Nagoya City University, 3–1, Tanabe-dori, Mizuho, Nagoya, Aichi 467–8603

A suspension of charged silica colloids was forced to flow in a flat capillary cell using an air-pulse-drive system. Above a critical air-pulse pressure, almost the entire capillary space was filled with a single-domain crystal with high spectral quality. The obtained flow-aligned particle arrays in water were immobilized as a self-standing hydrogel film using a photo-polymerization technique, thereby preserving the high quality. These results are basically the same as those for the previously reported polystyrene colloidal crystals, and they indicate that the present method is widely applicable to various kinds of particles.

Key-words : Colloidal crystals, Photonic crystals, Single crystal, Silica particle, Hydrogel

[Received February 1, 2010; Accepted February 18, 2010]

1. Introduction

Colloidal crystals are three-dimensional periodic arrays of monodisperse colloidal particles.[1)–5)] Their lattice spacing is usually in the order of submicrometers, resulting in the photonic band gap effect[6)–12)] in the visible or near-infrared light region. Therefore, they have potential applications in photonic crystals, optical filters, sensors, non-bleachable color materials, etc.[13)–18)] Although fabrication of a large-area single crystal is crucial for realizing such applications, it is usually time-consuming and difficult. We have developed a fast and simple process for fabricating a centimeter-sized single domain of colloidal crystals using a shear-induced method.[19),20)] A suspension of charged polystyrene colloids is forced to flow in a flat capillary cell. The strong shear flow generated in the cell induces a long-range orientational ordering of the crystals. The optical characterizations for the flow-aligned sample indicate that almost the entire capillary space (width: several square centimeters and thickness: 0.1 mm thick) is filled with a single-domain crystal with a fixed crystallographic orientation determined by the cell geometry.[19)–23)] Moreover, we have recently succeeded in immobilizing the obtained single-domain crystal, which is otherwise unstable against external disturbances such as mechanical vibrations and chemical contamination, as a self-standing hydrogel film using photo-polymerization while preserving the high optical quality.[24),25)]

Since our fabrication method mostly relies on the physical phenomenon of the shear-induced effect, we believe that our fabrication method is compatible with various kinds of particles. To date, various kinds of particles composed of ceramics, polymers, and metals have been prepared, and they have various uses such as magnets, semiconductors, and photocatalysts.[26)–34)] Therefore, experimental demonstration of the versatility of our method would be very significant in developing novel photonic crystals composed of such particles. In this paper, we examined the applicability of our method to colloidal silica particles, which are as widely used in this field as polystyrene. Silica has many advantages, including convenience and versatility.[35),36)] Silica particles having monodisperse size distribution are synthesized by the Stöber method[37)]; functional modification is also possible, e.g., synthesis of core-shell particles (functional particles covered with a silica layer)[38)] and mesoporous silica particles.[39)] Silica particles have weak-acid silanol groups on their surfaces as dissociable groups while polystyrene particles have strong acid groups. Therefore, the electrostatic interaction between silica particles is smaller than that of polystyrene particles although it is sufficiently strong to form the colloidal crystals. The density of silica is 2.1, which is twice as large as that of polystyrene. We examined the flow-induced single crystallization of the silica colloidal suspensions using the air-pulse-drive system. We also tried to immobilize the flow-aligned particle arrays without degrading the crystalline quality by using a photo-polymerization technique.

2. Experimental section

2.1 Single crystallization by shear flow

We used a suspension of uniform silica colloidal particles purchased from Nippon Shokubai Co., Ltd (KE-W20; particle diameter: 0.21 μm; standard deviation: 7%) without special treatments such as the surface modification of the particles and pH control of the suspension. The suspension, with a particle volume concentration of about 10%, was deionized in vials using mixed-bed ion-exchange resin (Bio-Rad, AG501-X8) until the suspension showed iridescence indicative of a crystal phase. The obtained poly-crystalline colloidal crystals were introduced into a flat capillary cell (thickness: 0.1 or 0.2 mm; width: 9 mm; length: 70 mm), and one side of the cell was connected to a digital pulse regulator (Musashi Engineering Inc., ML-606GX) with an air compressor (500 kPa maximum pressure) to apply an air pulse to the colloidal crystals in the cell (**Scheme 1**). Adjusting the air-pulse pressure (ΔP, difference from atmospheric pressure) quantitatively controlled the strength of the pulsed flow of the colloidal crystals. We processed various samples with different

† Corresponding author: T. Sawada; E-mail: SAWADA.Tsutomu@nims.go.jp

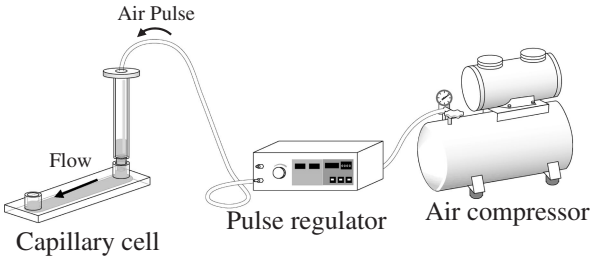

Scheme 1. Schematic diagram of the air-pulse-drive system for fabrication of uniform colloidal crystals.

ΔP values and investigated the flow effects on the crystalline texture as a function of ΔP.

2.2 Fixing the crystalline structure using a polymer gel

We used a poly(*N*-methylol acrylamide) gel to immobilize particle arrays. The colloidal suspension was mixed with aqueous solutions of *N*-methylol-acrylamide (N-MAM, 600 mM) as a monomer, *N*,*N*′-methylene-bis-acrylamide (BIS, 40 mM) as a crosslinker, and 2,2′-azobis[2-methyl-*N*-(2-hydroxyethyl)propionamide] (VA, 0.5 mM) as a photo-induced polymerization initiator for ultraviolet (UV) light. The reaction solution (particle volume concentration: about 10%) was bubbled with Ar gas for 10 min to remove dissolved O_2 and CO_2. It was then forced to flow in the capillary cell by the air-pulse-drive system to generate the shear-induced orientational ordering of the particles. The obtained flow-aligned particle arrays were immobilized by the photo-polymerization of the gelation agents in a UV light exposure chamber (Edmund Optics Inc., output power: 26 mW/cm^2 at 365 nm) for 30 min.

2.3 Characterization

The transmission spectra of the colloidal crystals were measured using a UV/VIS/NIR spectrophotometer (JASCO Corp., V-570), where the reference for the transmittance value was air. In order to check spatial uniformity in terms of the spectrum, the spatially resolved transmission spectra of the colloidal crystals were measured using an imaging spectrometer (ImSpector, JFE Techno-Research Corp.) for the wide sample area, with incident light normal to the cell surface and air as the reference. The red, green, and blue images (RGB-composed images) and single-wavelength images were taken at an in-plane image resolution of 100 × 25 microns. The particle arrangement immobilized in the gel film was observed using a scanning electron microscope (SEM), where the water in the gel film was replaced with ethylene glycol to slow the drying of the gel.

3. Results and discussion

Figure 1 shows the transmission spectra of the silica colloidal crystals processed with various ΔP values. The dip of the silica colloidal crystals is narrower and shallower than that of polystyrene colloidal crystals reported previously.[20] This is due to the decrease in the refractive index contrast between the particles and the surroundings.[9] (The refractive indices of the silica, polystyrene, and water are 1.45, 1.59, and 1.33, respectively.) The ΔP-dependent changes in the spectrum are basically the same as those of the polystyrene colloidal crystals; all samples show the deep dip at the stop band wavelength, and only the transmittance in the wavelength region shorter than the dip increases and then saturates with an increase in ΔP. This

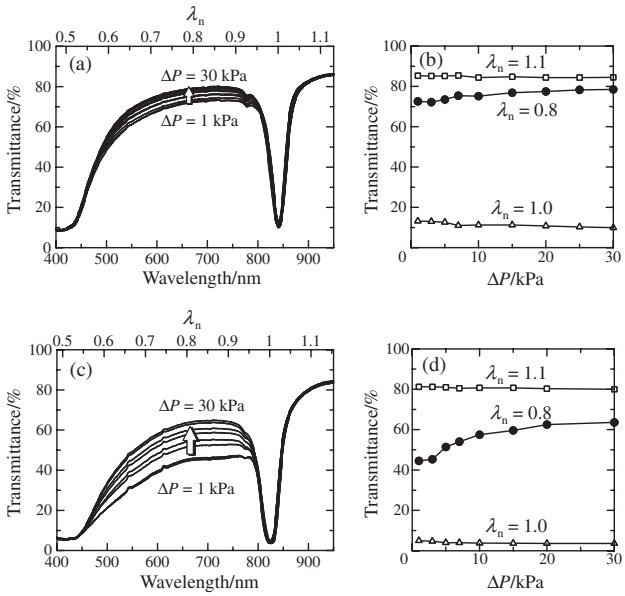

Fig. 1. (a) Transmission spectra of the silica colloidal crystals processed in the 0.1-mm-thick cell at various ΔP values. (b) ΔP-dependent changes in transmittance at representative wavelengths obtained from a. Here, λ_n represents a value normalized by the dip wavelength, $\lambda_n = \lambda/\lambda_{111}$. (c) Transmission spectra of the silica colloidal crystals processed in the 0.2-mm-thick cell at various ΔP values. (d) ΔP-dependent changes in transmittance at representative wavelengths obtained from c. The incident light is normal to the capillary face.

behavior indicates that the poly-crystalline domains of silica colloidal crystals can be aligned by increasing the flow rate according to the shear effect, as in the case of polystyrene. When compared with the polystyrene colloidal crystals, the transmittance change in silica colloidal crystals processed in the 0.1-mm-thick cell is very small (Fig. 1(a) and (b)). This is because the transmittance at $\Delta P = 1$ kPa is already a relatively high value of about 70%, where it almost reaches the saturation region. On the other hand, the transmittance of the silica sample processed in the 0.2-mm-thick cell shows a significant increase and saturation with an increase in ΔP (Fig. 1(c) and (d)), as in the case of the polystyrene sample processed in the 0.1-mm-thick cell. These results indicate that the silica particles have lower electrostatic interaction between particles than that of polystyrene particles, thereby generating stronger shear flow at the same air-pulse pressure. Hence, they can be aligned at a lower flow rate in the cell with the same thickness, and thicker crystals can be prepared at the same flow rate.

Figure 2(a) shows the transmission spectra of the flow-aligned silica colloidal crystals with gelation reagents processed in the 0.1-mm-thick cell before and after gelation. The spectrum before gelation (dashed line) shows the deep dip due to the stop band and high transmittance at the pass-band wavelength, indicating excellent optical quality. Under the appropriate polymerization conditions such as sufficient Ar bubbling, irradiation intensity, and time, the excellent quality of the transmission spectrum can be preserved after gelation, as shown by the solid line in Fig. 2(a). Figure 2(b) shows the spatial distribution of transmittance with brightness at three representative wavelengths below, at, and above the dip ($\lambda_n = 0.8$, 1.0, and 1.1), together with RGB-composed images for the same sample. The RGB images are equivalent to color photographs under transmission illumination from a white lamp. The sample has a yellowish

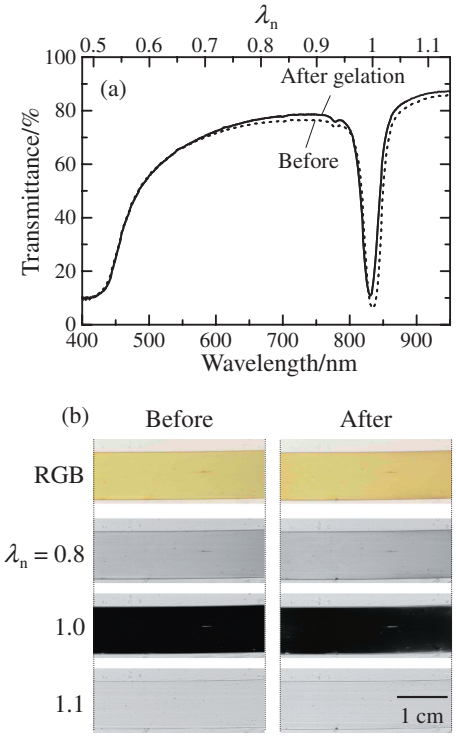

Fig. 2. (a) Transmission spectra of the flow-aligned colloidal crystals with gelation reagents before and after gelation. The cell thickness is 0.1 mm. (b) RGB-composed images and single-wavelength images taken under the transmission illumination before and after gelation. The incident light is normal to the capillary face.

Fig. 3. Photograph of the gel-immobilized silica colloidal crystal film soaked in water.

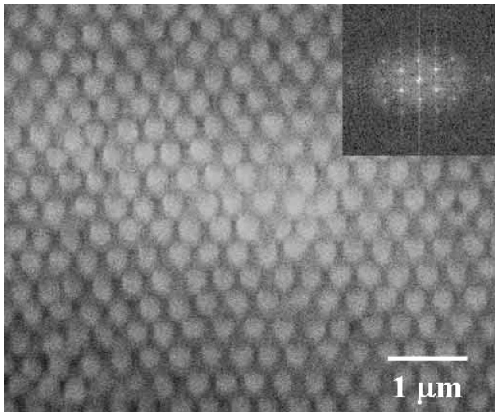

Fig. 4. SEM image of the top view of the gelled silica colloidal crystal film. The inset shows the Fourier transform of the image.

transmission color because it is transparent for wavelengths longer than approximately 500 nm, except for the dip, i.e., a lack of transmittance of the wavelength component for blue. For the single wavelength image, the absence of uniformity in the optical properties is detected on the basis of the contrast in brightness.[20),25)] These images indicate that the high uniformity over a large area is preserved after gelation. In general, fabrication of a uniform crystalline texture of colloidal particles with a high density is difficult since the sedimentation of particles readily degrades the texture. However, the present method can provide the uniform texture of silica particles despite their relatively high density of 2.1. This would be due to the fast preparation process of the present method; the shear-flow process is completed within 1 s and the following photo-polymerization takes several tens of minutes.

The obtained gel film is sufficiently solid to be handled with tweezers and can be removed from the fabrication cell as a self-standing film. **Figure 3** shows a photograph of the gel film soaked in water after being removed from the cell. The film thickness is about 0.1 mm, including over 300 particle layers along its thickness. Since the curved surface of the gel film is illuminated from various angles by using room lamps, it shows multiple iridescent colors. **Figure 4** shows the SEM image of the top view of the silica particle arrays immobilized in the hydrogel film and its Fourier transform. These images indicate that the silica particles are ordered well and exhibit a 6-fold symmetry. Large interparticle distance resulting from their electrostatic stabilization prior to gelation is evident. The crystal structure of the flow-aligned polystyrene colloidal crystals is a face-centered-cubic (fcc) structure, as reported previously.[20)] Since silica colloidal crystals have a wider crystalline region of a body-centered-cubic (bcc) structure in terms of particle concentration when compared with polystyrene, there is a possibility that the crystal structure of the flow-aligned silica colloidal crystals is bcc. However, the observed particle arrays have the 6-fold symmetry, as shown in Fig. 4. This indicates that they are not bcc structures which must exhibit a 2-fold symmetry. The hexagonal close-packed (hcp) arrays were originally thought to be arranged as ABCABC… (fcc structure), ABAB… (hcp structure), or randomly packed, all of which are difficult to be distinguished using SEM. In order to identify the three-dimensional structure, we measured the angle-dependent transmission spectra for the gel film (**Fig. 5**). These spectra show three dips (wavelengths λ_1, λ_2, and λ_3) that shift in the opposite directions as the incident angle changes. The angular dependence of Bragg wavelengths is calculated using the equation $\lambda_{air} = -2n_c S_0 G_{hkl}/|G_{hkl}|^2$. Here, λ_{air} is the Bragg wavelength in air; n_c, the refractive index of colloidal crystals; S_0, the unit vector parallel to the incident light in colloidal crystals; and G_{hkl}, the reciprocal vector of the *hkl* reciprocal lattice point. The refractive index of colloidal crystals n_c is assumed to be equal to the volume-weighted average of the refractive indices of the particles ($n_p = 1.45$) and the medium ($n_{md} = 1.33$), $n_c = n_p\phi + n_{md}(1 - \phi)$,[40)] where ϕ is the particle volume concentration. The incident angle in the colloidal crystals is corrected by applying Snell's law to consider refraction at the surface of the sample. As a result, it is consistently explained that λ_1 corresponds to 111 diffraction, λ_2 corresponds to 002 diffraction, and λ_3 corresponds to 200 and 020 diffractions from an fcc structure, as shown in Fig. 5(b). The dip λ_1 is also explained as the diffraction from the other structures, such as

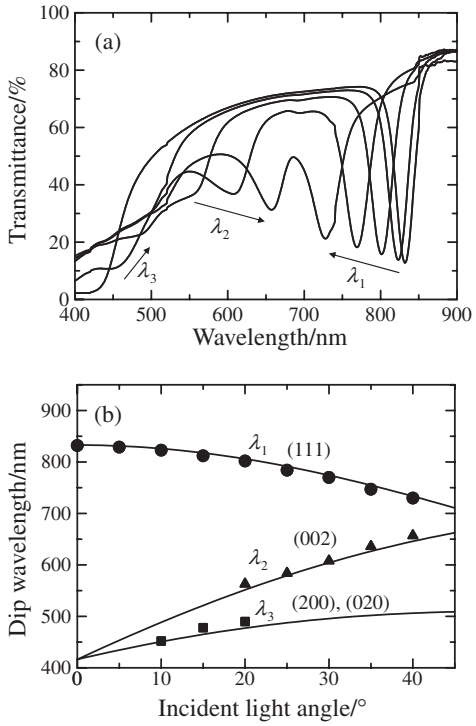

Fig. 5. (a) Angle-dependent transmission spectra of the gelled colloidal crystal film. The incident angle of the light is swung in the plane perpendicular to the capillary axis starting from the direction normal to the flat face of capillary to 40 deg. (b) Plots of the dip wavelength vs. incident light angle obtained from a. The solid line is the calculation curve obtained using the Bragg condition.

0002 diffraction from the hcp structure, 110 diffraction from the bcc structure, and the simple repetition of layers toward their normal direction. However, the dips λ_2 and λ_3 cannot be explained by structures other than the fcc structure. On the other hand, it should be noted that the flow-aligned colloidal crystals confined to the capillary cell do not necessarily have the same crystal structure as that in equilibrium, considering that the shear flow can induce structural changes in the charged colloids.[41] In the future, we intend to carry out a detailed studies of the flow-induced structural change in the present system.

4. Conclusion

We have examined the applicability of our method for fabricating a large-area gelled colloidal crystal film on silica colloidal particles. We found that the gelled silica colloidal crystal film with a high optical quality equivalent to that of a polystyrene colloidal crystal film can be fabricated by adjusting the fabrication conditions, even though silica particles have characteristics quite different from polystyrene particles. This result strongly suggests that the present method is applicable to various kinds of functional particles, and therefore can be used for industrial mass production of colloidal crystals and the development of novel colloidal photonic crystals.

References

1) P. Pieranski, *Contemp. Phys.*, **24**, 25–73 (1983).
2) K. Ito, K. Sumaru and N. Ise, *Phys. Rev. B*, **46**, 3105–3107 (1992).
3) N. Ise and M. V. Smalley, *Phys. Rev. B*, **50**, 16722–16725 (1994).
4) "Ordering and Phase Transitions in Charged Colloids," Ed. by A. K. Arora and B. V. R. Tata, VCH, New York (1996).
5) A. P. Gast and W. B. Russel, *Phys. Today*, **51**, 24–30 (1998).
6) E. Yablonovitch, *Phys. Rev. Lett.*, **58**, 2059–2062 (1987).
7) S. John, *Phys. Rev. Lett.*, **58**, 2486–2489 (1987).
8) J. D. Joannopoulos, R. D. Meade and J. N. Winn, "Photonic Crystals," Princeton University Press, Princeton NJ (1995).
9) K. Sakoda, "Optical Properties of Photonic Crystals," Springer-Verlag, Berlin (2001).
10) D. A. Weitz and W. B. Russel, Eds. *MRS Bull.*, **29**, 82–83 (2004).
11) A. Polman and P. Wiltzius, Eds. *MRS Bull.*, **26**, 608–610 (2001).
12) D. G. Grier, Ed. *MRS Bull.*, **23**, 21–21 (1998).
13) E. A. Kamenetzky, L. G. Magliocco and H. P. Panzer, *Science*, **263**, 207–210 (1994).
14) J. Holtz and S. A. Asher, *Nature*, **389**, 829–832 (1997).
15) O. D. Velev and E. W. Kaler, *Langmuir*, **15**, 3693–3698 (1999).
16) H. Fudouzi and Y. Xia, *Adv. Mater.*, **15**, 892–896 (2003).
17) S. H. Foulger, P. Jiang, A. Lattam, D. W. Smith, J. Ballato, D. E. Dausch, S. Grego and B. R. Stoner, *Adv. Mater.*, **15**, 685–689 (2003).
18) Y. Iwayama, J. Yamanaka, Y. Takiguchi, M. Takasaka, K. Ito, T. Shinohara, T. Sawada and M. Yonese, *Langmuir*, **19**, 977–980 (2003).
19) T. Sawada, Y. Suzuki, A. Toyotama and N. Iyi, *Jpn. J. Appl. Phys.*, **40**, L1226–L1228 (2001).
20) T. Kanai, T. Sawada, A. Toyotama and K. Kitamura, *Adv. Funct. Mater.*, **15**, 25–29 (2005).
21) T. Kanai, T. Sawada and K. Kitamura, *Langmuir*, **19**, 1984–1986 (2003).
22) T. Kanai, T. Sawada, I. Maki and K. Kitamura, *Jpn. J. Appl. Phys.*, **42**, L655–L657 (2003).
23) T. Kanai, T. Sawada and K. Kitamura, *Chem. Lett.*, **34**, 904–905 (2005).
24) A. Toyotama, T. Kanai, T. Sawada, J. Yamanaka, K. Ito and K. Kitamura, *Langmuir*, **21**, 10268–10270 (2005).
25) T. Kanai, T. Sawada, A. Toyotama, J. Yamanaka and K. Kitamura, *Langmuir*, **23**, 3503–3505 (2007).
26) Y. L. Li and T. Ishigaki, *Chem. Mater.*, **13**, 1577–1584 (2001).
27) B. Kim, S. L. Tripp and A. Wei, *J. Am. Chem. Soc.*, **123**, 7955–7956 (2001).
28) X. Xu, S. A. Majetich and S. A. Asher, *J. Am. Chem. Soc.*, **124**, 13864–13868 (2002).
29) C. Feldmann, *Adv. Funct. Mater.*, **13**, 101–107 (2003).
30) M. L. Breen, A. D. Dinsmore, R. H. Pink, S. B. Qadri and B. R. Ratna, *Langmuir*, **17**, 903–907 (2001).
31) K. P. Velikov, A. Moroz and A. van Blaaderen, *Appl. Phys. Lett.*, **80**, 49–51 (2002).
32) Y. Yin, Y. Lu, B. Gates and Y. Xia, *Chem. Mater.*, **13**, 1146–1148 (2001).
33) Y. Zhao, B. Sadtler, M. Lin, G. H. Hockerman and A. Wei, *Chem. Commun. (Camb.)*, 784–785 (2004).
34) T. Sugimoto, *Adv. Colloid Interface Sci.*, **28**, 65–108 (1987).
35) J. Yamanaka, M. Murai, Y. Iwayama, M. Yonese, K. Ito and T. Sawada, *J. Am. Chem. Soc.*, **126**, 7156–7157 (2004).
36) A. Toyotama, J. Yamanaka, M. Yonese, T. Sawada and F. Uchida, *J. Am. Chem. Soc.*, **129**, 3044–3045 (2007).
37) W. Stöber, A. Fink and E. Bohn, *J. Colloid Interface Sci.*, **26**, 62–69 (1968).
38) Y. S. Lin, Y. Hung, H. Y. Lin, Y. H. Tseng, Y. F. Chen and C. Y. Mou, *Adv. Mater.*, **19**, 577–580 (2007).
39) S. M. Yang, N. Coombs and G. A. Ozin, *Adv. Mater.*, **12**, 1940–1944 (2000).
40) P. A. Hiltner and I. M. Krieger, *J. Phys. Chem.*, **73**, 2386–2389 (1969).
41) B. J. Ackerson, *Nature*, **281**, 57–60 (1979).